Virchows Arch (2000) 436:336–344

ORIGINAL ARTICLE

**Christoph Röcken · Veit Hegenbarth · Maike Schmitz
Barbara Stix · Götz Schade · Andreas Mohnert
Albert Roessner**

Plasmacytoma of the tonsil with AL amyloidosis: evidence of post-fibrillogenic proteolysis of the fibril protein

Received: 14 September 1999 / Accepted: 29 October 1999

Abstract We report of a 58-year-old Caucasian man who was referred to the University Hospital with a greatly enlarged left tonsil which showed calcifications on computed-tomography scans. Histopathology revealed a plasmacytoma with secondary AL amyloidosis, ossifications, and multinucleated foreign-body-type giant cells. N-terminal sequencing of amyloid-fibril proteins purified from the formalin-fixed tissue showed the presence of two proteins of different size; these were of λ-light-chain origin (subgroup V), measured approximately 15.2 kDa and 10.5 kDa, and had identical N-terminal ends (YVLTQPP). When the amyloid deposits were immunolabeled with a polyclonal antibody directed against λ light chain, they showed two staining patterns: some deposits showed intense immunolabeling while others were not immunoreactive. Immunostaining of amyloid was completely absent after protease pre-treatment. Immunoelectron microscopy with gold-labeled secondary antibodies showed staining that was spatially related to amyloid fibrils and suggested that the antibody probably detected the fibril protein. Therefore, our hypothesis in this case is that the different immunostaining patterns are due to a post-fibrillogenic proteolysis of the fibril protein at the C-terminal end of the light chain, as indicated by the presence of two differently sized λ-light-chain fragments with identical N-terminal ends.

Key words Amyloid · λ Light chain · Osseous metaplasia · Plasmacytoma · Protease · Tonsil

C. Röcken (✉) · M. Schmitz · B. Stix · A. Roessner
Institute of Pathology, Otto-von-Guericke-University,
Leipziger Strasse 44, D-39120 Magdeburg, Germany
e-mail: christoph.roecken@medizin.uni-magdeburg.de
Tel.: +49-391-6713179, Fax: +49-391-6715818

V. Hegenbarth · G. Schade · A. Mohnert
Department of Otorhinolaryngology,
Otto-von-Guericke-University, Magdeburg, Germany

Introduction

Monoclonal immunoglobulin (Ig)-deposition diseases (MIDDs) are a group of disorders which feature the deposition of monoclonal proteins (M proteins) in organs and tissue, potentially causing disruption of organ function and/or organ failure. MIDDs are the result of clonal B-cell or plasma cell proliferation, and they may be either malignant, pre-malignant or non-malignant in nature. The proteins deposited are intact Ig or fragments thereof. The outcome of MIDD may not depend on the proliferation of B cells or plasma cells, but rather on the site and number of deposited M proteins that interfere with organ integrity. The deposits may be limited to certain organs, such as the kidneys in myeloma cast nephropathy or adult acquired Fanconi syndrome (AFS), or they may be more generalized, as in AL and AH amyloidosis, light-chain-deposition disease (LCDD), heavy-chain-deposition disease (HCDD), and light- and heavy-chain deposition disease (LHCDD) [9, 13, 29]. The M proteins may form fibrils, as in amyloidosis, or they may precipitate as granular deposits. Histopathologically, the type of MIDD can be determined by Congo-Red staining and ultrastructural analysis and by the presence of apolipoprotein E and amyloid P component. Apolipoprotein E and amyloid P component are commonly found in amyloid deposits, but are absent in LCDD, HCDD, and LHCDD [16, 17]. The type of MIDD probably depends on the type of protein (i.e., its primary structure) and certain host factors [9, 13, 29, 45]. Variable regions of κ light chain subclasses I and IV ($V\kappa_I$ and $V\kappa_{IV}$) are predominantly found in AFS and LCDD, whereas deposits of $V\lambda_{VI}$ are almost exclusively associated with AL amyloidosis [9, 13, 29]. Secondary structural modifications, such as glycosylation and limited proteolysis, may predispose M proteins to aggregate and deposit [9, 48].

Approximately 20% of patients with plasmacytoma suffer from secondary AL amyloidosis [1]. Tissue deposition of the M protein may occur at the tumor site or at a distance, in which case the precursor protein needs to be transported via bloodstream to the site of deposition.

Nevertheless, AL amyloidosis may be local or organ-limited, despite the presence of variable amounts of M protein in the serum. AL amyloidosis commonly involves the kidney (28% of cases), liver (24%), carpal ligament (21%), heart (17%), peripheral nerves (17%) and tongue (10%) [23]. Certain host factors, such as the metabolism of the M protein and its affinity for a particular organ structure or ligand (such as glycosaminoglycans or basement membrane proteins), may be involved in the process of deposition [13, 48]. Antibody–ligand interactions may also be responsible for selective organ involvement [48].

The clinicopathological presentation of patients with AL amyloidosis depends on the extent and distribution of the disease in addition to the cause. Specimens are frequently obtained from symptomatic organs, such as the kidney (in nephrotic syndrome) and the carpal ligament (in carpal tunnel syndrome) or by resection of a mass lesion where there is no clinical suspicion of amyloidosis and the pathologist is the first to consider and diagnose amyloidosis [42, 44]. We describe here the history of a patient who was admitted to the University Hospital with a greatly enlarged left tonsil which showed calcifications on computed tomography (CT) scan. The tonsil was subsequently found to be infiltrated by a plasmacytoma with secondary AL amyloidosis.

Clinical history

A 58-year-old Caucasian man was referred by his general practitioner to the Department of Otorhinolaryngology at the University Hospital. He complained of a foreign-body sensation in his throat and difficulty in swallowing that had persisted for 9 months. The past medical history of the patient included hypertension, which was treated with bisoprolol. He had been a smoker for 20 years and drank alcohol regularly. On admission, the patient was mobile, orientated in time, place and person, afebrile and normotonic, with a body weight of 88 kg and a height of 177 cm. Inspection of the oral cavity showed a greatly enlarged and indurated mobile left tonsil reaching beyond the middle line and the epiglottis. The mucosa covering the mass was intact. Bleeding on palpation was not apparent. A single indurated submandibular lymph node on the left site was palpable and measured approximately 2 cm in maximum diameter. The patient was not in heart failure. Blood tests showed mildly elevated erythrocyte-sedimentation rate (10 mm/1 h) and normal liver function test, urea and electrolytes and full blood count. Proteinuria was not found. Serum and urine electrophoresis and serum and urine immunofixation showed no monoclonal proteins. β2-Microglobulin and plasma viscosity were within normal limits. The electrocardiogram was normal. CT scans of the head and neck showed a 5×3.5×2.5-cm, well-demarcated lesion of the tonsil; this lesion enclosed hyperdense structures suggestive of calcifications (Fig. 1). On chest X-rays and CT scans of the chest, a small lesion measuring approximately 1 cm in greatest diameter was found in the right upper lobe of the lung. Bone lesions were not found on skeletal X-ray films. Ultrasound of the abdomen showed a benign renal cyst and no mass lesions in either the liver or kidneys. The spleen was not enlarged. A bone-marrow smear showed reactive changes with no evidence of plasmacytoma. A mild gastritis was found on oesophago-gastro-duodenoscopy. Rectoscopy showed a normal mucosal lining with no lesions. Finally, the left tonsil was resected suggesting the presence of either a malignant lymphoma or a lymphoepithelial carcinoma. The post-operative course was uncomplicated. Following diagnosis, the patient was referred to the Department of Hematology and Oncology for treatment.

Fig. 1 On computed-tomography scans, a large, well-demarcated lesion of the tonsil was found, which enclosed hyperdense structures suggestive of calcifications

Materials and methods

For light microscopy, the resected specimens from the tonsil and the gastric, duodenal and rectal biopsy specimens were fixed in formalin and embedded in paraffin. The samples from the bone-marrow biopsy were fixed in acetone and embedded in methacrylate. Sections were stained using hematoxylin and eosin, van Gieson's elastic stain, Giemsa's stain, and the periodic-acid Schiff (PAS) reaction. The presence of amyloid was demonstrated by the appearance of green birefringence due to alkaline, alcoholic Congo-Red staining under polarized light [37]. Immunostaining was performed with monoclonal antibodies directed against leukocyte common antigen (LCA; dilution 1:300), CD20 (1:200), CD68 (1:400), CD79a (1:50; all the preceding from Dako, Denmark), MiB1 (1:100; Dianova, Germany), IgA (1:15), IgG (1:50), IgM (1:30) and AA amyloid (1:500). Further immunostaining was performed using polyclonal antibodies directed against CD3 (1:150), lysozyme (1:10000), transthyretin (1:600), β2-microglobulin (1:2000), λ light chain (1:7500) and κ light chain (1:7500; all the preceding from Dako, Denmark). Prior to immunostaining, LCA, CD3, CD20, CD68, CD79a, MiB1, and transthyretin were pretreated with 10 mM ethylene diamine tetraacetic acid (EDTA; 2×10 min, 450 W microwave oven), λ- and κ light chains were treated with 0.5 U/ml protease I [16 min; according to manufacturer (Ventana, Strassbourg), this is a pronase from *Bacillus cereus*], and β2-microglobulin was treated with 0.1% papain (8 min). Immunostaining with anti-AA amyloid did not require specimen pretreatment. Immunoreaction was visualized using the avidin–biotin complex method with a Vectastain ABC alkaline-phosphatase kit (distributed by Camon, Wiesbaden, Germany) or an UltraTech HRP Streptavidin–Biotin Universal Detection System (Immunotech, Marseilles, France). Neufuchsin and 3,3-diaminobenzidine-tetrahydrochloride, respectively, served as chromogens. The specimens were counterstained with hematoxylin. The specificity of immunostaining was controlled using specimens containing known classes of amyloid (AA amyloid, transthyretin, β2-microglobulin), using positive controls recommended by the manufacturers for the remaining antibodies, and omitting the primary antibodies.

For electron microscopy (EM), specimens from the tonsil were fixed in a mixture of 2% formalin/2.5% glutaraldehyde (pH 7.2; overnight, 4ºC) and then in 3.125% glutaraldehyde (7 h, 4ºC). Following standard procedures of tissue processing for EM, the speci-

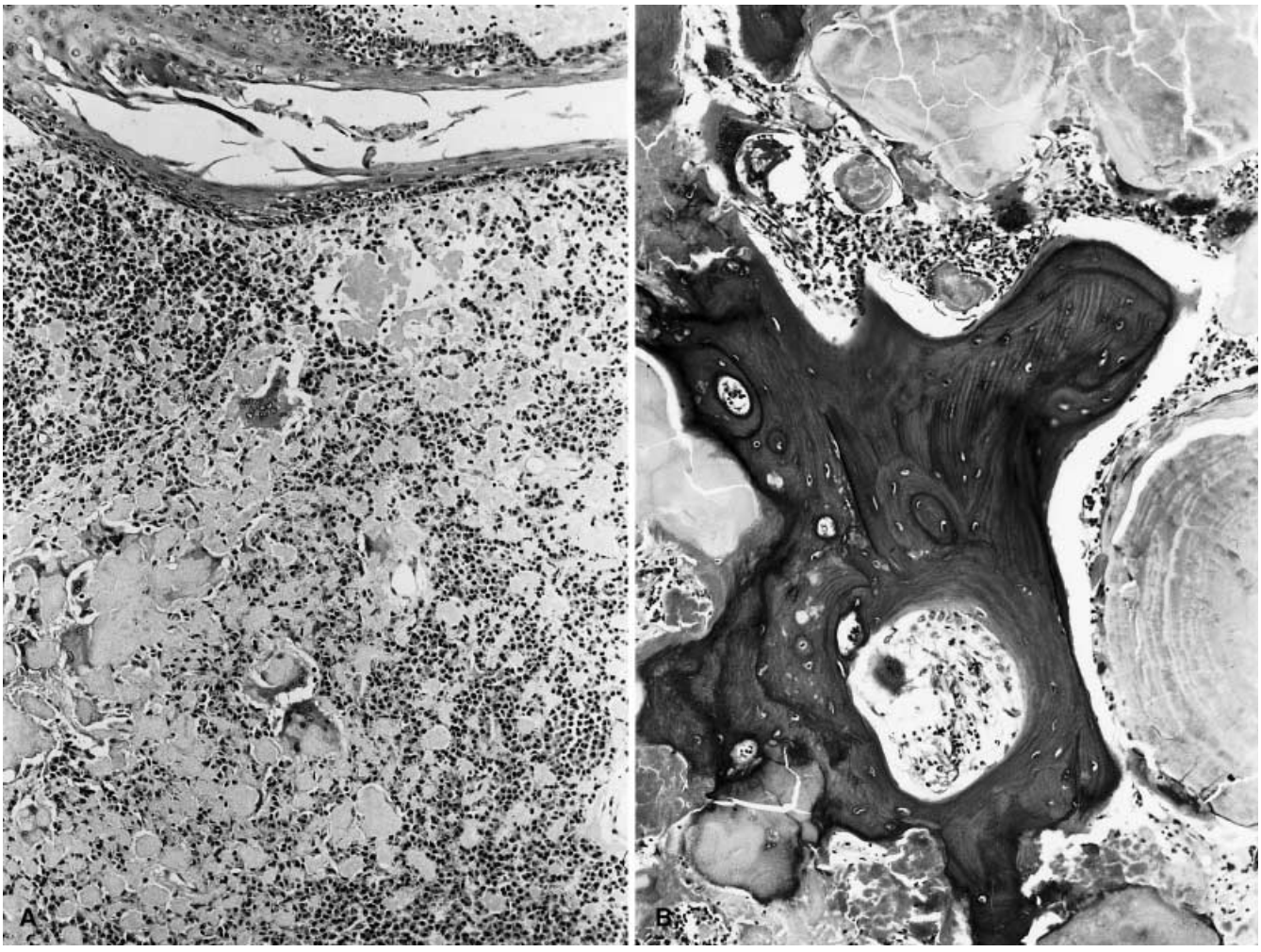

Fig. 2 The tonsil was infiltrated by a plasmacytoma with amyloid deposits (**A**), ossifications, and multinucleated foreign-body-type giant cells (**B**). Staining was performed using hematoxylin and eosin

mens were finally embedded in Epon-supplemented with 2% DMP-30. Polymerization took place over 24 h at 60°C. Semi-thin sections (1 µm) were stained with toluidine blue. Ultra-thin sections (80–120 nm) were mounted on copper grids and counterstained with 3% aqueous uranyl acetate [30 min, room temperature (rt)] and contrasted with 1% aqueous lead citrate (15 min, rt).

For post-embedding immunoelectron microscopy, ultra-thin sections (120 nm) were mounted on formvar-coated nickel grids (200 mesh; Plano, Wetzlar, Germany). The specimens were pretreated with 1 mM EDTA (pH 8.0; 30 min, 91ºC), as described elsewhere [41]; they were then rinsed in phosphate-buffered saline (PBS; pH 7.4, 3×5 min, rt) and incubated in PBS containing 5% (w/v) fetal calf serum (PBS-FCS; 30 min, rt). PBS-FCS was removed without washing the specimens, and antibodies directed against λ light chain (dilution 1:500; overnight, 4ºC) were applied. Immunostaining was visualized by EM with the appropriate 15-nm colloidal-gold-labeled secondary antibody [goat anti-rabbit IgG, 1:20 (BioTrend, Cologne, Germany); 60 min, rt]. Between the incubations, the specimens were washed with PBS-FCS (5×5 min). The antibodies were subsequently cross-linked with 1% glutaraldehyde in PBS (pH 7.4; 15 min, rt). Finally, the sections were counterstained with 3% aqueous uranyl acetate (30 min, rt) and contrasted with 1% aqueous lead citrate (15 min, rt). Fixation, staining and contrasting were each followed by extensive washing in distilled H_2O. The specificity of immunostaining was controlled by omitting the primary antibody. The sections were air dried and inspected in a Zeiss EM900 electron microscope.

The preparation of amyloid-fibril proteins from formalin-fixed specimens was performed as described by Layfield et al. [27]. In brief, this was performed as follows: 1.9 g of formalin-fixed tissue from the tonsil was incubated overnight in deionized water and was subsequently homogenized in five volumes of 50 mM Tris-HCl and 1 mM dithiothreitol (DTT; pH 7.5) for 2 min using an Ultra-Turrax T8-homogenizer with a 58N-8G dispersing tool from Windaus (IKA Labortechnik, Germany). The homogenate was centrifuged at 11,000 rpm for 14 min in an Eppendorf centrifuge 5403 (Eppendorf, Germany). The pellet was dissolved in 2.5 volumes of electrophoresis sample buffer [150 mM Tris-HCl,

Fig. 3 **A** Congo-red staining showed green birefringent amyloid deposits (B) which were not sensitive to protease pre-treatment. **C** Immunostaining with a polyclonal antibody directed against λ light chains showed intense labeling of the tumor cells and of the discrete interstitial deposits between tumor cells. **D** Immunostaining of amyloid is prevented by protease-I pre-treatment. Protease pre-treatment did not affect immunolabeling of the tumor cells. The large globular amyloid masses commonly encircled or infiltrated by multinucleated giant cells (C) showed scattered or no immunostaining, irrespective of whether or not protease pre-treatment was performed. Congo-red staining (A, B) and immunostaining with anti-λ light chain antibody (C, D) were performed without (A, C) and with (B, D) protease pre-treatment ▶

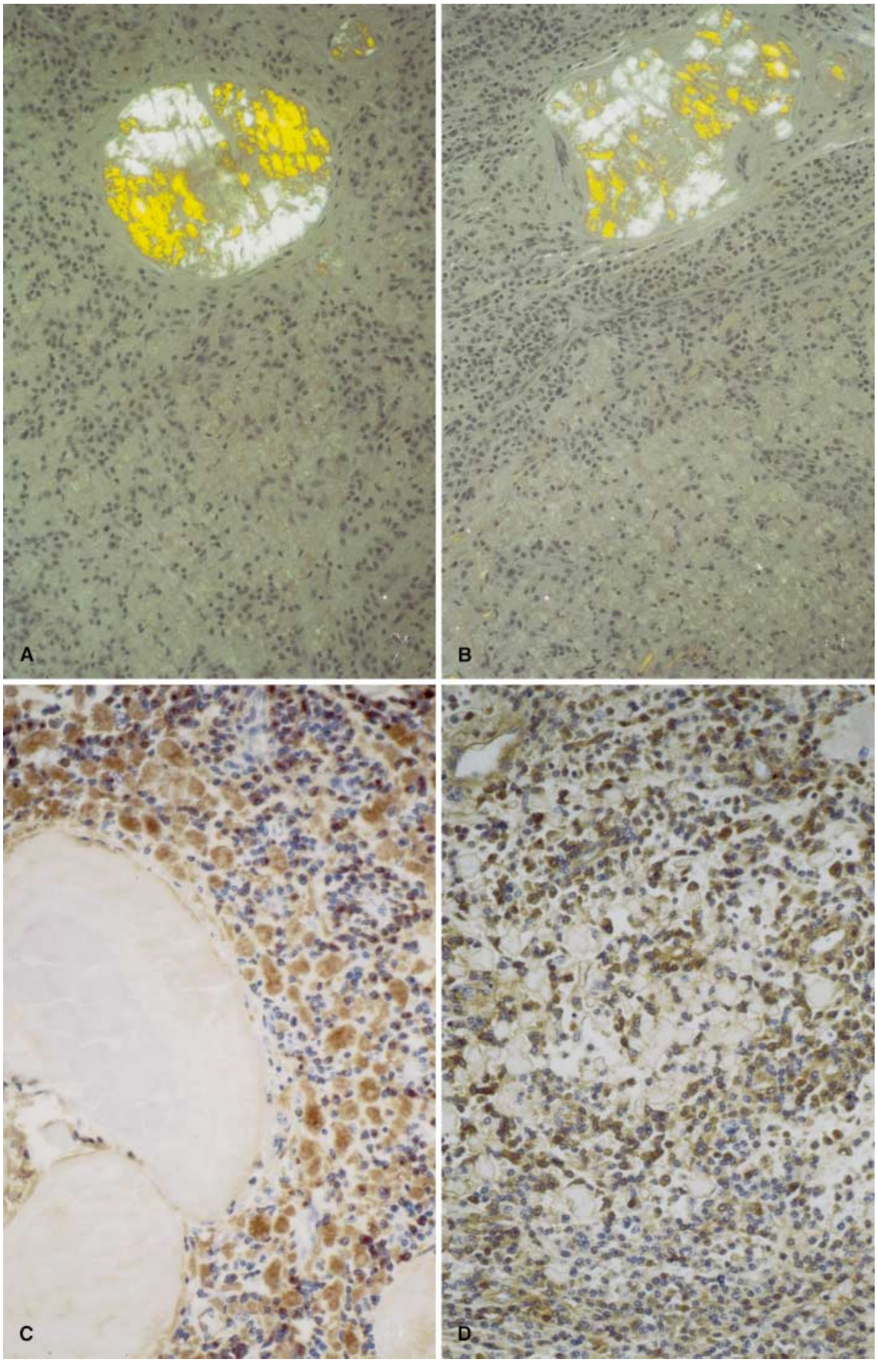
A
B
C
D

8 M urea, 2.5% (w/v) sodium dodecyl sulfate (SDS), 20% (v/v) glycerol, 10% (v/v) 2-β-mercaptoethanol and 2% (w/v) DTT, pH 6.8], heated to 90ºC for 20 min and again centrifuged at 11,000 rpm for 14 min. The protein concentration of the supernatant was estimated with the BioRad DC Protein assay kit (BioRad Laboratories, München, Germany). The supernatant containing the extracted protein was resolved by SDS polyacrylamide-gel electrophoresis (SDS-PAGE). Formalin-fixed specimens from an autopsy case with generalized AA amyloidosis served as positive controls [43].

Proteins were resolved according to the method of Laemmli [24] in 16% polyacrylamide gels and were visualized by staining with Coomassie blue or silver stain [30]. For Western blotting and amino acid sequencing, proteins on unstained polyacrylamide gels were transferred onto polyvinylidine-difluoride membranes [Immobilon-P^{SQ} (PVDF), pore size 0.1 µm; Millipore, Bedford, Mass.] using the tank-blotting system from BioRad Laboratories (München, Germany) according to the manufacturer's instructions. Transferred proteins were visualized by Coomassie-blue staining. Immunostaining of transferred proteins was performed using the Vectastain ABC alkaline-phosphatase kit (distributed by Camon, Wiesbaden, Germany) and antibodies directed either against AA-fibril protein (monoclonal, clone mc$_1$) or λ light chain (polyclonal; both compounds from Dakopatts, Denmark). Immunostaining was visualized with 5-bromo-4-chloro-3-indolyl phosphate/nitro blue tetrazolium salt (BioTrend Chemikalien GmbH, Köln, Germany). N-terminal amino acid sequencing was performed by WITA GmbH (Teltow, Germany). The protein was identified using "BLAST Sequence Similarity Searching", a program devised by the National Centre for Biotechnology Information.

Pathologic findings

The tonsillectomy specimen measured 6.0×4.0×2.0 cm and was covered by mucosa. The cut surface was firm, had ossifications and was gray in color.

Microscopically, the lymphatic tissue of the tonsil was almost completely replaced by infiltrates of tumor cells (Fig. 2A, Fig. 4A), which resembled mature plasma cells, and deposits of amorphous eosinophilic material, which encompassed almost 60% of the cross-sectional area. The tumor cells occasionally enclosed PAS-positive cytoplasmic inclusions and immunostained with antibodies directed against CD79a, λ light chain (Fig. 3C, D) and IgG but not with antibodies directed against LCA, CD3, CD20, κ light chain, IgA or IgM. Residual preexisting lymphatic tissue was scattered throughout, as indicated by immunostaining.

The amorphous eosinophilic material showed green birefringence in polarized light after Congo-Red staining and exhibited rigid fibrils of indefinite length and approximately 12 nm diameter on EM; both these features are characteristic for amyloid (Fig. 3B, Fig. 4D). Amyloid was present either as large globular masses (occasionally with a Maltese-cross-like birefringence) distributed diffusely throughout the specimen, discrete interstitial deposits between tumor cells or as scanty vascular deposits (Fig. 3A, B).

Areas of osseous metaplasia that were related spatially to amyloid deposits (Fig. 2B) and occasionally encircled them were found. Multinucleated CD68- and lysozyme-immunoreactive foreign-body-type giant cells were found surrounding amyloid deposits (Fig. 2, Fig. 4B) or apposed to the surface of the osseous metaplasia, suggestive of osteoclasts. Occasionally, they showed a vacuolated cytoplasm and asteroid bodies and immunostained for λ light chain and IgG. EM showed vesicles with fibrillar inclusions, which were similar to amyloid fibrils (Fig. 4C).

Immunostaining with a polyclonal antibody directed against λ light chain showed intense labeling of the discrete interstitial deposits between tumor cells; the deposits were only occasionally infiltrated by histiocytic cells (Fig. 3C). Immunostaining of amyloid was prevented by protease-I pre-treatment (Fig. 3D), but protease pre-treatment did not affect immunolabeling of the tumor cells (Fig. 3D). The large, globular amyloid masses, commonly encircled or infiltrated by multinucleated giant cells, showed scattered or no immunostaining, irrespective of whether protease pre-treatment was performed or not. Congo-Red staining was not influenced by protease pre-treatment (Fig. 3B). Post-embedding immunolabeling of amyloid using the antibody directed against λ light chain yielded immunostaining that was related spatially to amyloid fibrils (Fig. 4D).

Amyloid did not stain with antibodies directed against AA amyloid, transthyretin, β2-microglobulin or κ light chain (data not shown). Subsequent rectal biopsies showed scanty amyloid deposits in the submucosa. Amyloid was not observed in specimens from gastric, duodenal or bone-marrow biopsies. Gastric biopsy specimens showed a mildly chronic active gastritis caused by *Helicobacter pylori*. The biopsy of bone marrow did not show involvement by the plasmacytoma.

Figure 5 shows the material extracted from formalin-fixed tonsillar tissue after separation by SDS-PAGE. SDS-PAGE resolved five proteins, three of which had a molecular weight (MW) of 28 kDa or greater. These proteins probably do not represent monomeric fibril proteins, because none of the 18 different amyloid-fibril proteins so far characterized have a MW of 28 kDa or greater. However, two proteins were within the MW range commonly found for amyloid fibril proteins and weighed 15.2 kDa and 10.5 kDa. Western blotting with an antibody directed against λ light chain showed immunostaining of four bands (Fig. 6). Two immunoreactive bands were within the MW range of approximately 28 kDa or greater and probably represent intact light chains, which are found in virtually all AL amyloid extracts [48]. The other two immunoreactive bands had MWs of approximately 15.2 kDa and 10.5 kDa. No protein band was immunostained with a monoclonal antibody directed against AA amyloid-fibril proteins. The two proteins weighing 15.2 kDa and 10.5 kDa were submitted for N-terminal sequencing and showed identical N-terminal ends that were homologous to the variable region of λ light chain subgroup V; the N-terminal end of the upper band was YVLTQPPRVXVAP, and the lower band was YVLTQPP.

Material extracted from formalin-fixed splenic tissue of a patient suffering from generalized AA amyloidosis [43] served as a control and generated two bands at around

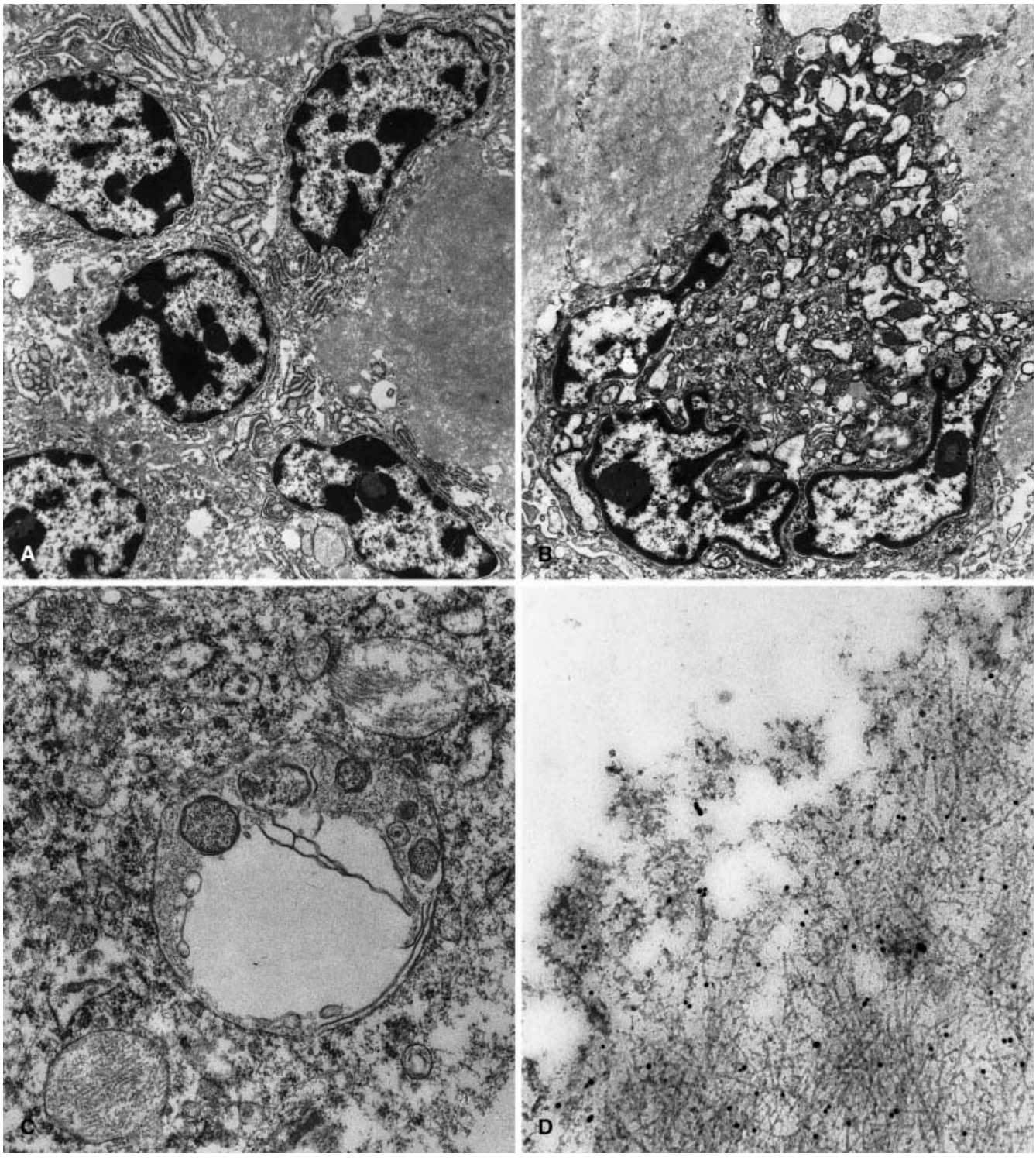

Fig. 4 Electron microscopy showed tumor cells with abundant rough endoplasmic reticulum and nuclear chromatin patterns, as is typical in plasmocytic cells (A; original magnification: ×3000), as well as multinucleated giant cells (B; original magnification: ×4400), some of which enclose vesicles with fibrillar inclusions similar to amyloid fibrils (C; original magnification: ×12,000). **D** Post-embedding immunolabeling of amyloid using the antibody directed against λ light chain yielded immunostaining related spatially to amyloid fibrils (original magnification: ×30,000)

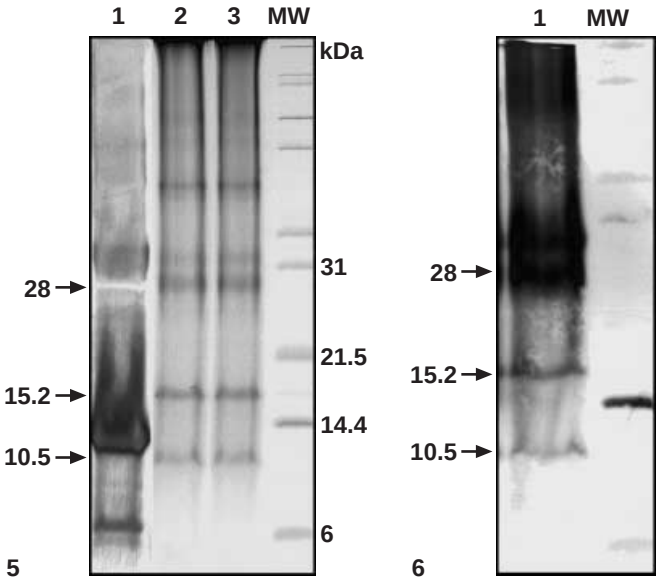

Fig. 5 Polyacrylamide-gel electrophoresis of material extracted from formalin-fixed tissue. *Lane 1*: precursor and fibril proteins extracted from formalin-fixed tissue of an autopsy case with known AA amyloidosis. Two proteins with a molecular weight of approximately 6 kDa were interpreted as monomeric AA-fibril proteins, and the protein with a weight of approximately 12 kDa was interpreted as serum amyloid A, as evidenced by Western blotting (data not shown). *Lanes 2 and 3*: material extracted from the tonsil. *MW* molecular-weight standards. Coomassie-blue staining was used

Fig. 6 Western blot with a polyclonal antibody directed against λ light chain, showing immunostaining of four bands of material extracted from the tonsil. Two bands have molecular weights of approximately 28 kDa or greater and probably represent intact light chains, and two bands have molecular weights of 15.2 kDa and 10.5 kDa, and are interpreted as fibril proteins. *Lane 1*: material extracted from the tonsil and immunostained with an antibody directed against λ light chain. *MW* molecular-weight standards

6 kDa and a broad band at approximately 12 kDa (Fig. 5); these bands were immunoreactive with a monoclonal antibody directed against AA amyloid (data not shown). These proteins were interpreted as monomeric AA-fibril proteins (the MW range was commonly 5–10 kDa) and serum amyloid A (approximately 12 kDa) [19].

Discussion

This case showed a plasmacytoma and massive deposition of amyloid in the tonsil. Since the tumor cells demonstrated λ-light-chain restriction and the amyloid-fibril protein was shown to be a fragment of the variable region of λ light chain subclass V ($V\lambda_V$), the MIDD observed in this case is interpreted as being AL amyloidosis secondary to a plasmacytoma. Since amyloid was also found in rectal biopsies, potential progression to a more generalized disease was apparent, and the lesion in the left upper lobe of the lung was finally interpreted as probable pulmonary involvement. The lack of evidence for a M protein in serum or urine is no contradiction to the diagnosis because, in 11% of the cases with AL amyloidosis, M protein is not found in either the serum or the urine [23].

Amyloid deposited in lymphatic tissue has been described (rarely) in the tonsil [2, 6, 7, 10, 14, 26, 31], is observed more frequently in lymph nodes and may be present in 6–23% of cases with generalized amyloidosis [8, 20, 25, 33, 34, 36, 38, 49]. From previous investigations, it appears that the tonsils and lymph nodes are mainly affected by AL amyloidosis and only occasionally by other forms, such as AA amyloidosis (15 versus two characterized cases) [2, 8, 20, 25, 33, 34, 49]. This may be due partly to the underlying disease which, as in our case, showed involvement of the lymphatic tissue and deposition of amyloid at the site of tumor progression. However, a sampling error cannot be excluded, because autopsy studies rarely investigate lymph-node involvement. Thus, participation of lymph nodes in forms of generalized amyloidosis other than AL amyloidosis may be underestimated [5, 18, 50]. The same reasoning may apply for amyloid affecting the tonsil, since no autopsy study has investigated the tonsils [3, 5, 12, 18, 36, 38, 50].

Both multinucleated giant cells and osseous metaplasia have been described as occurring in amyloid deposits, often showing an intimate spatial relationship with the deposits [15, 21, 28, 31, 35, 47, 52, 54]. However, their pathogenesis remains elusive. Where classification of the amyloid disease was performed, as in the present case, AL amyloidosis was identified more commonly than AA amyloidosis.

The presence of macrophages (M∅s) is a common finding in many different amyloid diseases, and it has been proposed that M∅s are involved in amyloidogenesis. They synthesize a broad range of proteases that may process the precursor protein, hence generating the fibril protein; they may also be involved in the degradation of the deposits [4, 11, 22, 32, 39, 40, 46, 51, 53].

In more then 95% of cases with AL amyloidosis, the deposits are composed of light-chain fragments [9], as found in this case. Protein fragmentation may be due to an abnormal λ or κ light-chain gene, aberrant protein synthesis, limited intracellular proteolysis of the precursor protein, post-secretory proteolysis or proteolysis after fibrillogenesis has occurred [9, 13, 48]. We observed fibrillar material in vesicles of the multinucleated histiocytic giant cells and found occasional immunostaining for IgG and λ light chain. This is a strong indication that, in our case histiocytic, cells participate in the disease process by either degrading or generating amyloid fibrils.

Immunolabeling of the amyloid deposits showed two staining patterns with a polyclonal antibody directed against λ light chain; some deposits were not immunoreactive at all (most commonly those that were surrounded by histiocytic cells), while others demonstrated intense immunolabeling. Since both were shown to be amyloid, as indicated by Congo-Red staining and EM, it is unlikely that different immunostaining patterns are related to

fibrillar (assembled in anti-parallel β-pleated sheets) and non-fibrillar (random) protein deposition. The preparation of the fibril proteins from formalin-fixed tissue showed two peptides of different sizes. N-terminal sequencing demonstrated that both peptides are fragments of $V\lambda_V$ and have identical N-terminal ends. The smaller protein differs from the larger one by loss of amino acids at the C-terminal end. Loss of these amino acids may cause loss of antigenicity in situ. Immunostaining of both proteins in vitro, as shown by Western blotting, does not contradict this assumption, because conformational changes and masking of antigens during the assembly of amyloid fibrils may alter staining characteristics in situ. Our observations may indicate that amyloid undergoes post-fibrillogenic processing, resulting in different immunostaining patterns and two proteins of different size. An observation in favor of this interpretation is that immunolabeling with anti-λ light chain was influenced by pre-treatment with protease I without affecting Congo-Red staining. Protease pre-treatment affected the antigenicity of amyloid but not the integrity of the fibril, which is important for Congophilia. The C-terminal residues of light-chain fibril proteins are typically located in sterically exposed regions of the molecule; these regions may be accessible for enzymatic cleavage by endoproteases [48].

Acknowledgements The authors thank Mrs. Becher, Mrs. Koçalkova, and Mrs. Mansfeld for their excellent and skilful assistance. This work was supported by grants from the Wilhelm Vaillant-Stiftung, München, Germany.

References

1. Alexanian R, Weber D, Liu F (1999) Differential diagnosis of monoclonal gammopathies. Arch Pathol Lab Med 123:108–113
2. Amado ML, Patino MJL, Blanco GL, Monreal FA (1996) Giant primary amyloidoma of the tonsil. J Laryngol Otol 110: 613–615
3. Antonutto G, Bartoli M, Melato M (1975) Histochemical study on systemic amyloid microdeposits with special reference to parathyroid intrafollicular deposits. Virchows Arch 368: 23–34
4. Arai K, Miura K, Baba S, Shirasawa H (1994) Transformation from SAA2-fibrils to AA-fibrils in amyloid fibrillogenesis: in vivo observations in murine spleen using anti-SAA and anti-AA antibodies. J Pathol 173:127–134
5. Baretton G, Linke RP, Löhrs U (1990) Systemische Amyloidosen. Immunhistochemische Typisierung an Autopsien mit Hilfe zahlreicher spezifischer Antikörper. Pathologe 11:71–79
6. Beiser M, Messer G, Samuel J, Gross B, Shanon E (1980) Amyloidosis of Waldeyer's ring. A clinical and ultrastructural report. Acta Otolarnygol (Stockh) 89:562–569
7. Benjamin I (1977) Pathologic quiz case 2. Amyloid nodule of the tonsil. Arch Otolaryngol (Stockh) 103:740–742
8. Boss JH (1993) Immunoglobulin-related amyloidosis presenting as recurrent isolated lymph node involvement. Arch Pathol Lab Med 117:870–870
9. Buxbaum J (1992) Mechanisms of disease: monoclonal immunoglobulin deposition. Hematol Oncol Clin North Am 6: 323–346
10. Chiari H (1937) Über isoliertes, lokales Amyloid in einer Tonsille. Monatsschr Ohrenheilkd Laryngorhinol 71:666–670
11. Chronopoulos S, Chan SL, Ratcliffe MJH, Ali-Khan Z (1995) Colocalization of ubiquitin and serum amyloid A and ubiquitin-bound AA in the endosomes-lysosomes: a double immunogold electron microscopic study. Amyloid 2:191–194
12. Cohen AS, Wills AA, III (1968) The incidence of amyloid deposits in 100 consecutive postmortem examinations. In: Mandema E, Ruinen L, Scholten JH, Cohen AS (eds) Amyloidosis: proceedings of the symposium on amyloidosis. Exerpta Medica, Amsterdam, pp 438–445
13. Dhodapkar MV, Merlini G, Solomon A (1997) Biology and therapy of immunoglobulin deposition diseases. Hematol Oncol Clin North Am 11:89–110
14. Eriksen HE (1970) A case of primary localized amyloidosis in both tonsils. J Laryngol Otol 84:525–531
15. Fasske E (1991) Tracheobronchopathia chondroosteoplastica mit Bronchusamyloidose und Bronchialkarzinom. Pathologe 12: 209–213
16. Gallo G, Picken MM, Frangione B, Buxbaum J (1988) Non-amyloidotic monoclonal immunoglobulin deposits lack amyloid P component. Mod Pathol 1:453–456
17. Gallo G, Wisniewski T, Choi-Miura NH, Ghiso J, Frangione B (1994) Potential role of apolipoprotein-E in fibrillogenesis. Am J Pathol 145:526–530
18. Hoshii Y, Takahashi M, Ishihara T, Uchino F (1994) Immunohistochemical classification of 140 autopsy cases with systemic amyloidosis. Pathol Int 44:352–358
19. Husby G, Marhaug G, Dowton B, Sletten K, Sipe JD (1994) Serum amyloid A (SAA): biochemistry, genetics and the pathogenesis of AA amyloidosis. Amyloid 1:119–137
20. Kahn H, Strauchen JA, Gilbert HS, Fuchs A (1991) Immunoglobulin-related amyloidosis presenting as recurrent isolated lymph node involvement. Arch Pathol Lab Med 115:948–950
21. Karasick D, Schweitzer ME, Miettinen M, O'Hara BJ (1996) Osseous metaplasia associated with amyloid-producing plasmacytoma of bone: a report of two cases. Skeletal Radiol 25: 263–267
22. Kreutzberg GW (1995) Microglia, the first line of defence in brain pathologies. Arzneimittelforschung 45:357–360
23. Kyle RA, Gertz MA (1995) Primary systemic amyloidosis: clinical and laboratory features in 474 cases. Semin Hematol 32 45–59
24. Laemmli UK (1970) Cleavage of structural proteins during the assembly of the head of bacteriophage T4. Nature 227:680–685
25. Lanzafame S, Magro G, Buffone N, Emmanuele C, Cirino E (1996) Localized primary amyloidosis of axillary lymph nodes. Histopathology 28:369–371
26. Lauritzen A (1987) Primary amyloidosis of the tonsil. Ugeskr Laeger 149:1539
27. Layfield R, Bailey K, Lowe J, Allibone R, Mayer RJ, Landon M (1996) Extraction and protein sequencing of immunoglobulin light chain from formalin-fixed cerebrovascular amyloid deposits. J Pathol 180:455–459
28. Lynch LA, Moriarty AT (1993) Localized primary amyloid tumor associated with osseous metaplasia presenting as bilateral breast masses: cytologic and radiologic features. Diagn Cytopathol 9:570–575
29. Maniatis A (1998) Pathophysiology of paraprotein production. Ren Fail 20:821–828
30. Merril LR, Goldman D, Sedman SA, Ebert MH (1981) Ultrasensitive stain for proteins in polyacrylamide gels shows regional variation in cerebrospinal fluid proteins. Science 211: 1437–1438
31. Michaels L, Hyams VJ (1979) Amyloid in localised deposits and plasmacytomas of the respiratory tract. J Pathol 128: 29–38
32. Miura K, Ju ST, Cohen AS, Shirahama TS (1990) Generation and use of site-specific antibodies to serum amyloid A for probing amyloid A development. J Immunol 144:610–613
33. Newland JR, Linke RP, Kleinsasser O, Lennert K (1983) Lymph node enlargement due to amyloid. Virchows Arch 399: 233–236

34. Newland JR, Linke RP, Lennert K (1986) Amyloid deposits in lymph nodes: a morphologic and immunohistochemical study. Hum Pathol 17:1245–1249
35. Olsen KE, Sletten K, Sandgren O, Olsson H, Myrvold K, Westermark P (1999) What is the role of giant cells in AL-amyloidosis. Amyloid 6:89–97
36. Pirani CL (1976) Tissue distribution of amyloid. In: Wegelius O, Pasternack A (eds) Amyloidosis. Academic, London, pp 33–49
37. Puchtler H, Sweat F, Levine M (1962) On the binding of Congo red by amyloid. J Histochem Cytochem 10:355–364
38. Ravid M, Gafni J, Sohar E, Missmahl HP (1967) Incidence and origin of non-systemic microdeposits of amyloid. J Clin Pathol 20:15–20
39. Röcken C, Kisilevsky R (1997) Binding and endocytosis of murine high density lipoprotein from healthy (HDL) and inflamed donors (HDL_{SAA}) by murine macrophages in vitro. A light- and electron-microscopic investigation. Amyloid 4:259–273
40. Röcken C, Kisilevsky R (1998) Comparison of the binding and endocytosis of high-density lipoprotein from healthy (HDL) and inflamed (HDL_{SAA}) donors by murine macrophages of four different mouse strains. Virchows Arch 432: 547–555
41. Röcken C, Roessner A (1999) An evaluation of antigen retrieval procedures for immunoelectron microscopic classification of amyloid deposits. J Histochem Cytochem 47:1385–1394
42. Röcken C, Schwotzer E, Linke RP, Saeger W (1996) The classification of amyloid deposits in clinicopathological practice. Histopathology 29:325–335
43. Röcken C, Wieker K, Grote HJ, Müller G, Franke A, Roessner A (2000) Rosai-Dorfman disease and generalized AA amyloidosis. A case report. Hum Pathol (in press)
44. Saeger W, Röcken C (1998) Amyloid: mikroskopischer Nachweis, Klassifikation und klinischer Bezug. Pathologe 19: 345–354
45. Schiffer M (1996) Molecular anatomy and the pathological expression of antibody light chains. Am J Pathol 148:1339–1344
46. Shirahama TS, Cohen AS (1975) Intralysosomal formation of amyloid fibrils. Am J Pathol 81:101–116
47. Sidoni A, Alberti PF, Bravi S, Bucciarelli E (1998) Amyloid tumours in the soft tissues of the legs. Case report and review of the literature. Virchows Arch 432:563–566
48. Solomon A, Weiss DT (1995) Protein and host factors implicated in the pathogenesis of light chain amyloidosis (AL amyloidosis). Amyloid 2:269–279
49. Spitale LS, Jimenez DB, Montenegro RB (1998) Localised primary amyloidosis of inguinal lymph node with superimposed bone metaplasia. Pathology 30:321–322
50. Strege RJ, Saeger W, Linke RP (1998) Diagnosis and immunohistochemical classification of systemic amyloidoses. Report of 43 cases in an unselected autopsy series. Virchows Arch 433:19–27
51. Takahashi M, Yokota T, Kawano H, Gondo T, Ishihara T, Uchino F (1989) Ultrastructural evidence for intracellular formation of amyloid fibrils in macrophages. Virchows Arch 415: 411–419
52. Yamada M, Hatakeyama S, Yamamoto E, Kimura Y, Tsukagoshi H, Yokota T, Uchino F (1988) Localized amyloidosis of the uterine cervix. Virchows Arch 413:265–268
53. Yamada M, Itoh Y, Shintaku M, Kawamura J, Jensson O, Thorsteinsson L, Suematsu N, Matsushita M, Otomo E (1996) Immune reactions associated with cerebral amyloid angiopathy. Stroke 27:1155–1162
54. Yokoo H, Nakazato Y (1998) Primary localized amyloid tumor of the breast with osseous metaplasia. Pathol Int 48: 545–548